also been demonstrated [19]. An alternative hypothesis is that there is an accumulation of saliva in the mouth during the contraction, which may increase the conductivity between the electrodes, causing a decrease in SEMG amplitude.

V. Conclusion

A new GG SEMG electrode array has been designed, and its performance evaluated in ten healthy subjects. The compact acrylic appliance clips in place over the mandibular teeth and incorporates two linear arrays of embedded pin electrodes which make contact with the mucosa above the two genioglossus muscles. Using this electrode it is possible to estimate GG CV as well as GG SEMG amplitude and frequency parameters in a range of conditions despite the difficulty posed by several anatomical and environmental factors particular to the study of this important muscle. The best GG SEMG signals for GG CV estimation were recorded from the middle of the array, using electrodes 6, 9, and 12 mm posterior to the lingual gingival wall. The estimated CV was independent of force level during short contractions at forces between 40%–100% MVC, but a significant decrease in estimated CV was observed during fatiguing contraction at 50% MVC, accompanied by a decrease in the median frequency of the power spectrum. Interestingly there was also a decrease in the RMS amplitude of the GG SEMG, which may suggest inhomogeneous behavior. These results highlight the need for further investigation into the function of the GG using SEMG, in both normal subjects and patients with OSAS, which may exhibit altered GG function. The new appliance design now provides a sensor for measuring GG muscle fiber CV, which offers the possibility of assessing GG function with increased insight.

References

[1] T. Young, M. Palta, J. Dempsey, J. Skatrud, S. Weber, and S. Badr, "The occurrence of sleep-disordered breathing among middle-aged adults," *N. Engl. J. Med.*, vol. 328, no. 17, pp. 1230–1235, 1993.

[2] M. Carrera, F. Barbe, J. Sauleda, M. Tomas, C. Gomez, C. Santos, and A. G. N. Agusti, "Effects of obesity upon genioglossus structure and function in obstructive sleep apnoea," *Eur. Respir. J.*, vol. 23, no. 3, pp. 425–429, Mar. 2004.

[3] P. C. Deegan and W. T. McNicholas, "Pathophysiology of obstructive sleep apnoea," *Eur. Respir. J.*, vol. 8, no. 7, pp. 1161–1178, Jul. 1995.

[4] R. Merletti, D. Farina, and M. Gazzoni, "The linear electrode array: A useful tool with many applications," *J. Electromyogr. Kinesiol.*, vol. 13, no. 1, pp. 37–47, Feb. 2003.

[5] R. Merletti, M. Knaflitz, and C. J. D. Luca, "Myoelectric manifestations of fatigue in voluntary and electrically elicited contractions," *J. Appl. Physiol.*, vol. 69, no. 5, pp. 1810–1820, Nov. 1990.

[6] E. A. Doble, J. C. Leiter, S. L. Knuth, J. A. Daubenspeck, and D. Bartlett, Jr, "A noninvasive intraoral electromyographic electrode for genioglossus muscle," *J. Appl. Physiol.*, vol. 58, no. 4, pp. 1378–82, 1985.

[7] J. Cullen, M. Lowery, W. T. McNicholas, P. Nolan, M. J. O'Malley, and C. O'Muircheartaigh, "Optimisation of electrode design to detect myoelectric manifestations of fatigue in the human genioglossus muscle," presented at the XXXIV Int. Conf. Physiological Sciences, Christchurch, New Zealand, 2001.

[8] C. M. O'Connor, L. Doherty, P. Nolan, and M. O'Malley, "Measurement of muscle fiber conduction velocity in the human genioglossus muscle," in *Proc. 1st Int. IEEE EMBS Conf. Neural Engineering*, Capri, Italy, 2003, pp. 392–395.

[9] P. R. Eastwood, G. T. Allison, K. L. Shepherd, I. Szollosi, and D. R. Hillman, "Heterogeneous activity of the human genioglossus muscle assessed by multiple bipolar fine-wire electrodes," *J. Appl. Physiol.*, vol. 94, no. 5, pp. 1849–1858, 2003.

[10] M. S. McHugh, J. Cullen, P. Nolan, and M. J. O'Malley, "Muscle force and EMG measurement in an upper airway muscle," in *Proc. XVIIth ISB Congr.*, Calgary, AB, Canada, 1999, pp. 883–883.

[11] M. Naeije and H. Zorn, "Estimation of the action potential conduction velocity in human skeletal muscle using the surface EMG cross-correlation technique," *Electromyogr. Clin. Neurophysiol.*, vol. 23, no. 1-2, pp. 73–80, Jan. 1983.

[12] C. J. D. Luca, "Physiology and mathematics of myoelectric signals," *IEEE Trans. Biomed. Eng.*, vol. BME-26, pp. 313–325, Jun. 1979.

[13] R Development Core Team, "R: A Language and Environment for Statistical Computing," R Foundation for Statistical Computing, Vienna, Austria, 2005, ISBN 3–9000051–07–0. [Online]. Available: http://www.R-project.org

[14] J. Pinheiro, D. Bates, S. DebRoy, and D. Sarkar, nlme: Linear and Nonlinear Mixed Effects Models. R package version 3.1-57, 2005.

[15] K. C. McGill and L. J. Dorfman, "High-resolution alignment of sampled waveforms," *IEEE Trans. Biomed. Eng.*, vol. BME-31, pp. 462–468, 1984.

[16] D. Farina and R. Merletti, "A novel approach for estimating muscle fiber conduction velocity by spatial and temporal filtering of surface EMG signals," *IEEE Trans. Biomed. Eng.*, vol. 50, no. 12, pp. 1340–1351, Dec. 2003.

[17] R. B. Beck, C. J. Houtman, M. J. O'Malley, M. M. Lowery, and D. F. Stegeman, "A technique to track individual motor unit action potentials in surface EMG by monitoring their conduction velocities and amplitudes," *IEEE Trans. Biomed. Eng.*, vol. 52, no. 4, pp. 622–629, Apr. 2005.

[18] Zijdewind, D. Kernell, and C. G. Kukulka, "Spatial differences in fatigue-associated electromyographic behaviour of the human first dorsal interosseus muscle," *J. Physiol.*, vol. 483, pt. 2, pp. 499–509, Mar. 1995.

[19] S. Tsuiki, T. Ono, Y. Ishiwata, and T. Kuroda, "Functional divergence of human genioglossus motor units with respiratory-related activity," *Eur. Respir. J.*, vol. 15, no. 5, pp. 906–10, 2000.

Methods of Solving Reduced Lead Systems for Inverse Electrocardiography

Alireza Ghodrati*, Dana H. Brooks, and Robert S. MacLeod

***Abstract*—In the context of inverse electrocardiography, we examine the problem of using measurements from sets of electrocardiographic leads that are smaller than the number of nodes in the associated geometric models of the torso. We compared several methods to estimate the solution from such reduced-lead measurements sets both with and without knowledge of prior statistics of the measurements. We present here simulation results that indicate that deleting rows of the forward matrix corresponding to the unmeasured leads performs best in the absence of prior statistics, and that Bayesian (or least-squares) estimation performs best in the presence of prior statistics.**

***Index Terms*—Inverse electrocardiography, lead selection, reduced lead-sets.**

I. Introduction

Choosing the number and placement of body-surface electrodes, along with how best to apply data from a smaller number of electrodes to a forward model built from a much larger number of computation nodes, remain important questions for wider clinical application of

Manuscript received October 20, 2005; revised July 14, 2006. This work was supported in part by the Whitaker Foundation, in part by the Nora Eccles Treadwell Foundation and the Richard A. and Nora Eccles Harrison Fund for Cardiovascular Research, and in part by the Center for Integrative Biomedical Computing (CIBC), National Institutes of Health (NIH), NCRR, under project 2-P41-1RR12553-07. *Asterisk indicates correpsonding author.*

*A. Ghodrati is with the Department of Algorithm Development, Draeger Medical, Andover, MA 01810 USA (e-mail: alireza.ghodrati@draeger.com).

D. H. Brooks is with the Communications and Digital Signal Processing Center, Department of Electrical and Computer Engineering, Northeastern University, Boston, MA 02115 USA (e-mail: brooks@ece.neu.edu).

R. S. MacLeod is with The Nora Eccles Harrison Cardiovascular Research and Training Institute (CVRTI), Bioengineering Department, and Scientific Computing and Imaging (SCI) Institute, University of Utah, Salt Lake City, UT 84112 USA (e-mail: macleod@cvrti.utah.edu).

Digital Object Identifier 10.1109/TBME.2006.886865

inverse electrocardiography. Here, we report on an examination of several approaches for using data collected at fewer than the full set of computational nodes. In particular, we study three methods to address the question of solving a reduced lead system.

A. Problem Formulation

We use the epicardial potential distribution as our source model, and solve the forward problem using a typical Boundary Element Method [1]. We formalize this relationship as

$$\mathbf{y} = \mathbf{A}\mathbf{x} + \mathbf{n} \tag{1}$$

where $\mathbf{y}$ is an $M \times 1$ vector of torso surface potentials at a particular time instant, $\mathbf{A}$ is the $M \times N$ forward matrix, $\mathbf{x}$ is an $N \times 1$ vector that holds the heart surface potentials at a particular time instant, and $\mathbf{n}$ represents measurement noise. For simplicity, we find the inverse solution separately at each time instant and take the torso to be homogenous. Because of the attenuation and smoothing effects of the body, the forward matrix $\mathbf{A}$ is ill-conditioned [2] and requires regularization. Here, we use a standard Tikhonov approach [3]

$$\widehat{\mathbf{x}}_{\boldsymbol{\lambda}} = (\mathbf{A}^{\mathrm{T}}\mathbf{A} + \boldsymbol{\lambda}^{2}\mathbf{R}^{\mathrm{T}}\mathbf{R})^{-1}\mathbf{A}^{\mathrm{T}}\mathbf{y} = \mathbf{A}_{\boldsymbol{\lambda}}^{\dagger}\mathbf{y} \tag{2}$$

where λ is the regularization parameter, $\mathbf{R}$ is a regularization matrix, and $\mathbf{A}_{\boldsymbol{\lambda}}^{\dagger}$ represents the $N \times M$ regularized "inverse operator" matrix based on $\mathbf{A}$ at a particular value of λ. In the sequel, we assume that the identity matrix $\mathbf{I}$ is used for the regularizer $\mathbf{R}$.

The problem we address is: assume we have only K measurements, $K < M$. What is the best way to use those K measurements to estimate $\widehat{\mathbf{x}}_{\lambda}$ in the context of (2)? We describe and evaluate three different solutions to this problem.

B. Method I: Row Deletion

The most common approach in the literature has been to delete the rows of the forward matrix corresponding to the unmeasured leads; it minimizes the regularized residual only over the nodes for which measurements are available, ignoring the rest. Thus the reduced forward matrix has K rows. We can formalize the row removal process as premultiplication of $\mathbf{A}$ by a $K \times M$ matrix $\mathbf{T}$, where $\mathbf{T}$ is a selection matrix with one "1" in each row in the column corresponding to the selected row of $\mathbf{A}$ and all other elements zero, $\mathbf{A}_{\mathbf{s}} = \mathbf{T}\mathbf{A}$, and the measured data is then $\mathbf{y}_{\mathbf{s}} = \mathbf{T}\mathbf{y}$. The Tikhonov regularization mechanism of (2) leads to

$$\widehat{\mathbf{x}}_{\mathbf{s},\boldsymbol{\lambda}} = (\mathbf{A}^{\mathrm{T}}\mathbf{T}^{\mathrm{T}}\mathbf{T}\mathbf{A} + \boldsymbol{\lambda}^{2}\mathbf{I})^{-1}\mathbf{A}^{\mathrm{T}}\mathbf{T}^{\mathrm{T}}\mathbf{T}\mathbf{y} = \mathbf{A}_{\mathbf{s},\boldsymbol{\lambda}}^{\dagger}\mathbf{y}_{\mathbf{s}} \tag{3}$$

where the definition of $\widehat{\mathbf{x}}_{\mathbf{s},\lambda}$ follows from that of $\mathbf{A}_{\mathbf{s}}$, λ, and $\mathbf{y}_{\mathbf{s}}$.

C. Method II: Column Deletion

In this approach, we first compute the $N \times M$ inverse matrix $\mathbf{A}_{\boldsymbol{\lambda}}^{\dagger}$, then delete columns corresponding to the $(M - K)$ unmeasured nodes, leading to

$$\widehat{\mathbf{x}}_{\mathbf{c},\boldsymbol{\lambda}} = (\mathbf{A}^{\mathrm{T}}\mathbf{A} + \boldsymbol{\lambda}^{2}\mathbf{I})^{-1}\mathbf{A}^{\mathrm{T}}\mathbf{T}^{\mathrm{T}}\mathbf{T}\mathbf{y} = \mathbf{A}_{\boldsymbol{\lambda}}^{\dagger}\mathbf{T}^{\mathrm{T}}\mathbf{y}_{\mathbf{s}}. \tag{4}$$

D. Method III: Estimation

Column deletion implicitly assumes that the potentials at the unmeasured nodes are all zero; a better estimate of those potentials than zero might lead to a better solution. Hence, a third method is to estimate the data at the unmeasured nodes from those at the measured nodes and then solve the full inverse problem. We investigated this approach using two estimation methods, Laplacian interpolation [4] and Bayesian (least-squares) estimation [5].

1) Estimation by Laplacian Interpolation: Following Oostendorp *et al.* [4], we find the potentials of the unmeasured nodes to minimize the 2-norm of the surface Laplacian of the torso potentials over all M nodes. This method has been verified by different groups for body surface interpolation [6], [7]. It leaves the measured values unchanged, adjusting only the values at the unmeasured nodes to make the result "maximally smooth" in the 2-norm of the approximate Laplacian sense. This resulting inverse solution is

$$\widehat{\mathbf{x}}_{\mathrm{L}} = \mathbf{A}_{\lambda}^{\dagger}\widehat{\mathbf{y}}_{\mathrm{L}} \tag{5}$$

where $\widehat{\mathbf{y}}_{\mathrm{L}}$ has both measured leads and Laplacian interpolated potentials.

2) Bayesian Estimation: The Bayesian method[1] uses the mean and covariance of the full set of torso potentials $\mathbf{y}$ to estimate the unknown potentials such that the mean square error between the estimated and (unknown) true potentials at all nodes is minimized. This is a standard estimation technique [8] which has been used to estimate body surface potentials from sparse measurements [5] and recently to estimate activation times from a sparse set of venous catheter electrodes [9]. The mean and full covariance matrix of the torso potentials are not directly available; the usual approach is to derive them from a training set of high resolution measurement [5], [6]. The inverse solution then becomes

$$\widehat{\mathbf{x}}_{\mathrm{B}} = \mathbf{A}_{\lambda}^{\dagger}\widehat{\mathbf{y}}_{\mathrm{B}} \tag{6}$$

where $\widehat{\mathbf{y}}_{\mathrm{B}}$ contains the measured leads plus the Bayesian estimated potentials.

3) Implementation: For the Bayesian method, we estimated the mean vector and covariance matrix of the torso measurements from a training set. The covariance matrix was estimated as $\widehat{\mathbf{C}}_{\mathbf{y}} = (1/P)\sum_{i=1}^{P}(\mathbf{y_i} - \overline{\mathbf{y}})(\mathbf{y_i} - \overline{\mathbf{y}})^{\mathrm{T}}$, where P is the total number of time instants across all beats in the training set, $\mathbf{y_i}$ represents the ith torso potential sample in the set, and $\overline{\mathbf{y}} = (1/P)\sum_{\mathbf{i=1}}^{\mathbf{P}}\mathbf{y_i}$. Since it would be difficult to obtain a training set of data for all M geometric nodes, we assumed the training set was known only for the 192-lead configuration (Fig. 1) typically employed at the Cardiovascular Research and Training Institute (CVRTI) and estimated $\widehat{\mathbf{C}}_{\mathbf{y}}$ based on those nodes. Using the Bayesian method, we estimated the torso potentials at the unmeasured leads of this 192-lead set from the measured leads. Then we used the row deletion method to obtain a forward matrix corresponding to this 192-lead configuration for use in the inverse solution. We used a similar procedure for the Laplacian interpolation method, interpolating just to the same 192 lead locations. This allowed us to compare Laplacian and Bayesian approaches under the same conditions.

E. Experimental Methods

We used epicardial potentials measured at the CVRTI from a canine heart that had been placed in a tank built to simulate an adolescent human torso. Measurements were taken at 490 sites on the heart surface using a sock electrode [10]. Our full forward solution had $M = 771$, so that $\mathbf{A}$ was 771×490. We simulated torso measurements from the measured heart data using the forward matrix and added white Gaussian noise at an SNR of 30 dB before computing inverse solutions. For the Bayesian method estimation of the mean vector and covariance

[1]We note that this is always the minimum mean square error linear estimate, but only the Bayes estimate with appropriate Gaussianity assumptions.

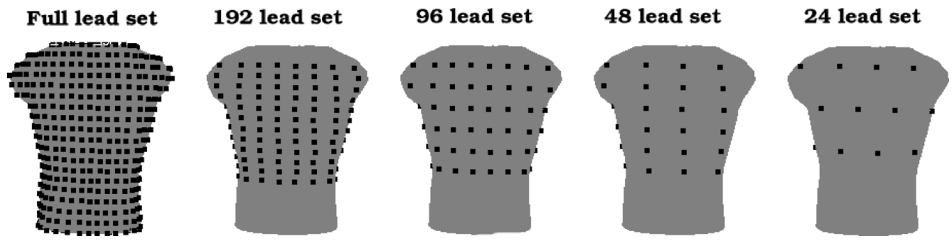

Fig. 1. Regularly distributed lead configurations used in the simulations.

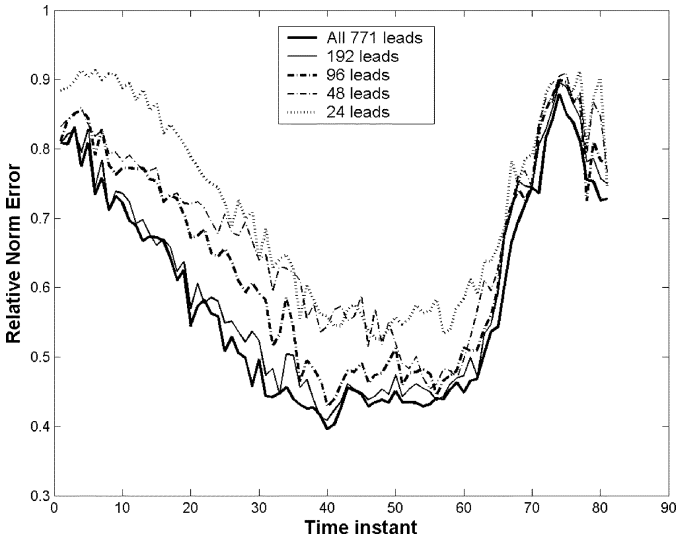

Fig. 2. Relative error norm during QRS for regularly distributed lead sets using row deletion for a left ventricle paced beat.

matrix of the 192-lead torso measurements was carried out using data from 470 heartbeats from different animals with different pacing sites [9]. Inverse solution results were obtained using the proposed methods on data from five heartbeats not in the training set, paced on both the right and left ventricles.

1) Comparison Metrics: We used both visual examination of isopotential maps and a relative error norm defined as $RE = \|\mathbf{x} - \widehat{\mathbf{x}}_\lambda\|_2 / \|\mathbf{x}\|_2$, where $\mathbf{x}$ is the true solution and $\widehat{\mathbf{x}}_\lambda$ is the regularized inverse solution, to compare our results to the measured epicardial data.

2) Lead Set Selection: Since the problem of selecting the best leads is itself a large subject [11]), we used regularly distributed 24-, 48-, and 96-lead subsets of the 192 electrodes typically employed at the CVRTI. We emphasize these lead sets are used to compare the performance of the proposed methods and the leads are not placed at the optimum locations in terms of the inverse solutions. We also used the theoretical "full" lead set of 771 nodes from the forward-computed torso data. Fig. 1 illustrates these different lead configurations.

3) Parameter Selection: The regularization parameter for the zero order Tikhonov regularization was chosen to minimize the norm of the error between the regularized solution and the true solution to avoid complicating the results with additional errors due to regularization parameter selection.

II. Unified Statistical Framework

We found it useful to compare the solutions presented above within a unified statistical framework. We start by observing that the inverse solution using a Bayesian method for a zero-mean Gaussian random variable $\mathbf{x}$ is [8]

$$\widehat{\mathbf{x}} = (\mathbf{A}^{\mathbf{T}}\mathbf{C}_{\mathbf{n}}^{-1}\mathbf{A} + \mathbf{C}_{\mathbf{x}}^{-1})^{-1}\mathbf{A}^{\mathbf{T}}\mathbf{C}_{\mathbf{n}}^{-1}\mathbf{y} \tag{7}$$

where $\mathbf{C_n}$ and $\mathbf{C_x}$ are the measurement noise and solution covariance matrices, respectively. In this framework, the Tikhonov solution is a special case in which both measurement noise and solution are assumed to be zero-mean and white with covariances $\sigma_n^2\mathbf{I}$ and $\sigma_x^2\mathbf{I}$, respectively. The regularization parameter then would be σ_n^2/σ_x^2. Starting from (7), we can find equivalent statistical assumptions that lead to the inverse solutions introduced by each of the three-lead reduction methods.

A. Row Deletion Method

Comparing (7) with (3), it is apparent that they are equivalent as long as the solution has a zero-mean white Gaussian distribution with covariance $\sigma_x^2\mathbf{I}$, while the measurement noise is zero-mean Gaussian with inverse covariance matrix $\sigma_n^{-2}\mathbf{T}^{\mathbf{T}}\mathbf{T}$. Matrix $\mathbf{T}^{\mathbf{T}}\mathbf{T}$ is diagonal with diagonal elements corresponding to the measured leads equal to one and the rest equal to zero. We observe that in effect the noise variances at the unmeasured nodes are assumed to be infinite, i.e., they are not trusted and contribute nothing to the solution.

B. Column Deletion Method

Comparing (7) with (4) in the statistical framework, reveals that measurements noise and the solution are both assumed to have zero-mean and white Gaussian distributions with inverse covariances $\sigma_n^{-2}\mathbf{I}$ and $\sigma_x^{-2}\mathbf{I}$, as in the full Tikhonov solution, but the measurement vector becomes $\mathbf{T}^{\mathbf{T}}\mathbf{T}\mathbf{y}$, equivalent to assuming a zero value for all unmeasured nodes. In this case, the measurement noise covariance assumes the same noise power for the measured and unmeasured nodes regardless of the possible large error in the unmeasured values which are set to zero.

C. Estimation

Comparing (7) with either (6) or (5) reveals that the assumptions are similar to that of the column deletion approach but likely with better estimates for unmeasured nodes. Implicit in this result is an assumption that the noise power for the measured nodes and unmeasured nodes are the same, which seems rather inaccurate. In any case, the accuracy of the solution would depend on the accuracy of the estimation or interpolation schemes. If knowledge of the additional variance due to the estimation is available, this result suggests that it could indeed be incorporated into the estimation procedure.

III. Results

We show results for one beat, paced on the left ventricle; results were similar for the other beats tested. Fig. 2 shows inverse solution relative

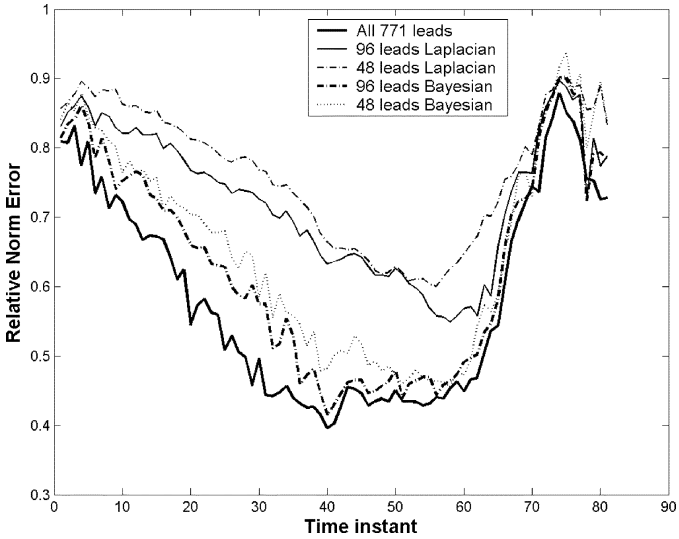

Fig. 3. Relative error norm during QRS for regularly distributed lead sets using Laplacian and Bayesian interpolation for a left ventricle paced beat.

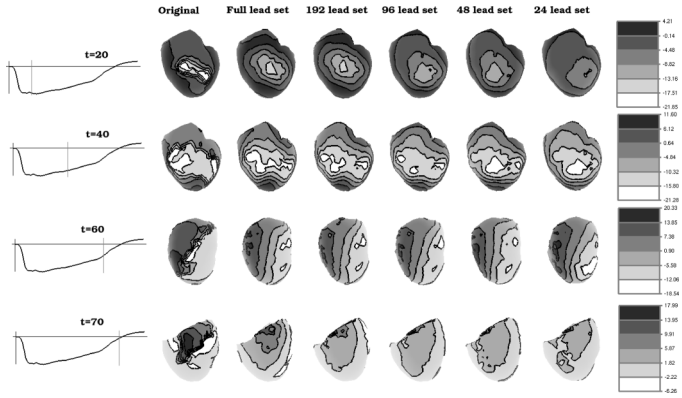

Fig. 4. Potential maps of original data and inverse solutions for reduced lead sets for four time instants. Inverse solution were obtained by row deletion. Contours show iso-potential lines. The left column shows an electrogram close to the pacing site. The right column shows the color map of each row. The time instant of each row is marked on the time signal and its timing given in milliseconds with respect to the pacing time.

error versus time during the QRS interval, using row deletion, for different numbers of leads. We note that the increase in error with a decreasing number of leads was not very large, especially for lead sets with 96 or more leads. Fig. 3 shows similar results for Laplacian and Bayesian estimations for 96 and 48 leads only, along with the results using data from all 771 nodes. The Laplacian interpolation method was more sensitive to decreased number of leads than either row deletion or Bayesian estimation. Errors using Bayesian and row deletion methods were comparable for the 96- and 48-lead sets. We omit results from the column-deletion approach because they showed much larger errors than the other methods, (*e.g.,* the RE with 96 leads was never less than 0.85). Potential maps from 4 time instants for different lead configurations are shown using row deletion in Fig. 4 and both Bayesian estimation and Laplacian interpolation in Fig. 5. The same value-to-color mapping were used on all maps and contours show iso-potential lines. The left column shows an electrogram close to the pacing site; the time instant of each row is marked on the corresponding electrogram. Times shown are in milliseconds with respect to pacing. The plots were drawn with the *map3d* software [12].

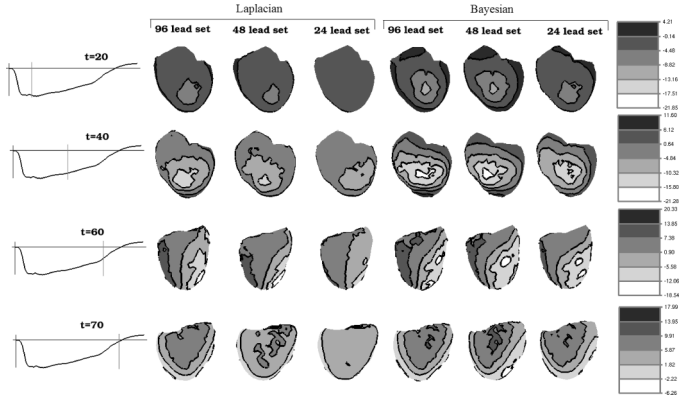

Fig. 5. Potential maps of inverse solutions for reduced lead sets for 4 time instants. Inverse solution were obtained by the Laplacian interpolation and the Bayesian estimation methods. Same format as previous figure.

Fig. 4 is typical for the row deletion method in its ability to preserve most of the features from the full lead-set solution, such as the elliptical shape of the wavefront and the location of activated areas of the epicardium. Although early after activation ($t = 20$) the shape of the reconstructed wavefront was more circular than elliptical with 96 and fewer leads, at ($t = 40$) and later the elliptical shape was evident even in the small lead sets. Fig. 5 shows that with Laplacian interpolation the wavefront was circular even at ($t = 40$) with 96 leads, and the potential map was highly smoothed (less dense contours); thus, localization of the activated area was poor. In contrast, Bayesian estimation preserved these features quite well even with the smallest lead set. This supports other reports that the Bayesian method performed better than the Laplacian method for interpolating torso potentials for small lead sets [6].

IV. Discussion

The relatively poor performance of column deletion, compared to row deletion, is perhaps not surprising considering our statistical analysis, which shows that this method places equal confidence on assumed zero values for the unmeasured nodes as on the measurements themselves, since the inverse problem is ill-posed and, thus, highly sensitive to measurement errors. Laplacian interpolation to "restore" unmeasured values did not generally perform as well as simple row deletion; important features of the solution were lost, especially for small lead sets, despite the fact that the torso potential map is generally smooth. This likely is due to a large interpolation error for small lead sets, combined again with ill-posedness. Our statistical analysis suggests that if the estimation variance of the interpolation error were taken into consideration one might achieve a more reliable result. The Bayesian method used a covariance matrix estimated from a training set which did not include the test beats. The fact that results with this method were the best of those tested, at least in terms of relative error, in particular for small lead sets, suggests that if reasonably accurate covariance matrices can be obtained by study of an appropriate set of prior subjects, this may be the method of choice. However, the isopotential maps were quite similar between row deletion and the Bayesian method, so it is not completely clear that the effort of obtaining the covariance would be justified. We also note that in practice, torso shapes will vary among subjects, a complexity not represented in our tank simulations. Thus, the improvement predicted using the covariance matrix in our simulations may be overly optimistic. In the absence of highly reliable and specific prior assumptions, our simulations suggest that it may be generally better to apply the row deletion approach, i.e., to remove the

rows of the forward matrix corresponding to the unmeasured nodes and solve the system with the new forward matrix.

Our results also indicate the presence of considerable redundant information in torso surface measurements with regards to obtaining good quality inverse solution. However, such an inference should be considered in the context of the specifics of this experiment, i.e., using zero order Tikhonov solutions and simulated torso measurements. The redundant information found in our experiment may indeed turn out to be valuable for reconstructions in a different context, when real torso measurements are used and, thus, forward model error would play a role. In our study, we effectively removed any influence from the forward model error. We speculate that the Bayesian estimation method might be more robust in the presence of such error than the row deletion method because of its use of prior information.

ACKNOWLEDGMENT

The authors gratefully acknowledge B. Yilmaz for preparation of the training set of ECG data used in this paper.

REFERENCES

[1] R. C. Barr, M. Ramsey, and M. S. Spach, "Relating epicardial to body surface potential distributions by means of transfer coefficients based on geometry measurements," *IEEE Trans. Biomed. Eng.*, vol. BME-24, no. 1, pp. 1–11, Jan. 1977.

[2] Y. Rudy and B. J. Messinger-Rapport, "The inverse problem in electrocardiography: Solutions in terms of epicardial potentials," *CRC Crit. Rev. Biomed. Eng.*, vol. 16, no. 3, pp. 215–268, 1988.

[3] P. C. Hansen, *Rank-Deficient and Discrete Ill-Posed Problems*. Philadelphia, PA: SIAM, 1997.

[4] T. F. Oostendorp, A. van Oosterom, and G. Huiskamp, "Interpolation on a triangulated 3D surface," *J. Comput. Phys.*, vol. 80, no. 2, pp. 331–343, 1989.

[5] R. L. Lux, C. R. Smith, R. F. Wyatt, and J. A. Abildskov, "Limited lead selection for estimation of body surface potential maps in electrocardiography," *IEEE Trans. Biomed. Eng.*, vol. BME-25, no. 3, pp. 270–276, May 1978.

[6] R. Hoekema, G. J. Uijen, D. Stilli, and A. van Oosterom, "Lead system transformation of body surface map data," *J. Electrocardiol.*, vol. 31, no. 2, pp. 71–82, 1998.

[7] R. S. MacLeod, R. L. Lux, and B. Taccardi, "Translation of body surface maps between different electrode configurations using a three-dimensional interpolation scheme," in *Proc, Int. Congr. Electrocardiology, XXth Annu. Meeting*, 1993, pp. 179–182.

[8] S. M. Kay, *Fundamentals of Statistical Signal Processing: Estimation Theory*. Upper Saddle River, NJ: Prentice-Hall, 1993.

[9] B. Yılmaz, R. S. MacLeod, B. B. Punske, B. Taccardi, and D. H. Brooks, "Venous catheter based mapping of ectopic epicardial activation: training data set selection for statistical estimation," *IEEE Trans. Biomed. Eng.*, vol. 52, no. 11, pp. 1823–1831, Nov. 2005.

[10] R. S. MacLeod, Q. Ni, B. Punske, P. R. Ershler, B. Yilmaz, and B. Taccardi, "Effects of heart position on the body-surface ECG," *J. Electrocardiol.*, vol. S33, pp. 229–237, 2000.

[11] A. Ghodrati, "Lead selection and wavefront-based models for the inverse problem of electrocardiography," Ph.D. thesis, Electrical Engineering, Northeastern Univ., Boston, MA.

[12] R. S. MacLeod and C. R. Johnson, "Map3d: Interactive scientific visualization for bioengineering data," in *Proc. IEEE Engineering in Medicine and Biology Soc. 15th Annu. Int. Conf.*, 1993, pp. 30–31.